

Lennart Crona, Mattias Karlsson, Peter Krylstedt, Johan Mattsson

# Marine electromagnetic characterisation and analysis of 3D environmental effects

SWEDISH DEFENCE RESEARCH AGENCY

Systems Technology  
SE-172 90 Stockholm

FOI-R—1461--SE

November 2004

ISSN 1650-1942

**Technical report**

Lennart Crona, Mattias Karlsson, Peter Krylstedt, Johan Mattsson

# Marine electromagnetic characterisation and analysis of 3D environmental effects

<b>Issuing organization</b> FOI – Swedish Defence Research Agency Systems Technology SE-172 90 Stockholm	<b>Report number, ISRN</b> FOI-R—1461--SE	<b>Report type</b> Technical report
	<b>Research area code</b> 43 Underwater Sensors	
	<b>Month year</b> November 2004	<b>Project no.</b> E6051
	<b>Sub area code</b> 43 Underwater Sensors	
	<b>Sub area code 2</b>	
<b>Author/s (editor/s)</b> Lennart Crona Mattias Karlsson Peter Krylstedt Johan Mattsson	<b>Project manager</b> Per Söderberg	
	<b>Approved by</b> Monica Dahlén	
	<b>Sponsoring agency</b> Swedish armed forces	
	<b>Scientifically and technically responsible</b> Peter Krylstedt	
<b>Report title</b> Marine electromagnetic characterisation and analysis of 3D environmental effects		
<b>Abstract (not more than 200 words)</b> <p>Inversion of electromagnetic sub-bottom parameters and 3D modelling of the bottom topography is presented in this paper. In particular, horizontally stratified conductivity profiles are determined from space- and frequency-sounding data collected at a controlled electromagnetic (CEM) source experiment in the southern Stockholm archipelago conducted in June 2004. The inversion, of the piecewise continuous conductivity profiles, is formulated as an optimisation problem. A restarted local Levenberg-Marquardt search algorithm is used to determine the sub-bottom conductivity profile that minimises the differences between measured and numerical data. The obtained results, for a specific part of the trial site, are compared with inverted profiles from a similar field trial performed in August 2002 in the same area. Especially, the impact from the seasonal variation in the seawater conductivity profile on the estimated sub-bottom profiles is indicated.</p> <p>Finally, effects from the bottom topography on the electric field when a source is towed along a track are investigated and modelled. A volume integral equation technique is used to model the non-planar part of the track. It is shown that the variations in the electric field amplitude due to different water depths along the track can be accurately modelled by using an extended Born approximation approach. The electric field amplitude is increased as much as 14 dB compared to a horizontally stratified bottom at the most shallow part of the track. Hence, the detection capability for an electric sensor system is increased when sources passes shallow parts of an area or close to island.</p>		
<b>Keywords</b> Marine electromagnetics, environmental characterisation, inversion, 3D modelling		
<b>Further bibliographic information</b>	<b>Language</b> English	
<b>ISSN</b> 1650-1942	<b>Pages</b> 14 p.	
	<b>Price acc. to pricelist</b>	

<b>Utgivare</b> Totalförsvarets Forskningsinstitut - FOI Systemteknik 172 90 Stockholm	<b>Rapportnummer, ISRN</b> FOI-R—1461--SE	<b>Klassificering</b> Teknisk rapport
	<b>Forskningsområde</b> 4. Ledning, informationsteknik och sensorer	
	<b>Månad, år</b> November 2004	<b>Projektnummer</b> E6051
	<b>Delområde</b> 43 Undervattenssensorer	
	<b>Delområde 2</b>	
<b>Författare/redaktör</b> Lennart Crona Mattias Karlsson Peter Krylstedt Johan Mattsson	<b>Projektledare</b> Per Söderberg	
	<b>Godkänd av</b> Monica Dahlén	
	<b>Uppdragsgivare/kundbeteckning</b> Försvarsmakten	
	<b>Tekniskt och/eller vetenskapligt ansvarig</b> Peter Krylstedt	
<b>Rapportens titel (i översättning)</b> Marin elektromagnetisk miljökaraktärisering och analys av 3D effekter		
<b>Sammanfattning (högst 200 ord)</b> <p>Inversion av elektromagnetiska bottenparametrar samt 3D modellering av botten-topografi beskrivs i denna rapport. Speciellt uppskattas planskiktade profiler, av den elektriska ledningsförmågan från botten och neråt, med hjälp av uppmätta elektriska fält från ett rums- och frekvenssonderingsexperiment i södra Stockholms skärgård under juni månad 2004. Inversionen av de styckvis kontinuerliga ledningsförmågaprofilerna formuleras som ett optimeringsproblem. En återstartad lokal sökmetod baserad på en Levenberg-Marquardt algoritm används för att bestämma den fysikaliskt korrekta profil som minimerar skillnaden mellan mätdata och numerisk data. De erhållna resultaten jämförs med motsvarande resultat från ett tidigare försök i samma område. Inverkan av olika säsongsberoende ledningsförmågaprofiler i vattnet med avseende på de uppskattade bottenledningsförmågorna indikeras.</p> <p>Slutligen undersöks effekten på de elektriska fälten i en bottenplacerad sensor när en elektrisk strömdipolkälla bogseras längs en löpa med varierande topografi. En volymsintegralekvationsmetod används för att modellera den icke plana delen av löpan. Variationerna i amplituden hos det elektriska fältet på grund av olika vattenedjup längs löpan kan beräknas med god noggrannhet. Längs löpan förstärks amplituden vid uppgrunningarna. Vid det grundaste stället ökar amplituden med 14 dB jämfört med numerisk data från en plan bottenmodell. Det betyder att detektionskapaciteten för ett elektriskt sensorsystem ökar när en källa passerar grunda delar av ett område eller rör sig nära land.</p>		
<b>Nyckelord</b> Marin elektromagnetik, miljökaraktärisering, inversion, 3D-modellering		
<b>Övriga bibliografiska uppgifter</b>	<b>Språk</b> Engelska	
<b>ISSN</b> 1650-1942	<b>Antal sidor:</b> 14 s.	
<b>Distribution enligt missiv</b>	<b>Pris:</b> Enligt prislista	

## **Contents**

<b>1 Introduction</b>	<b>5</b>
<b>2 The field trial</b>	<b>5</b>
<b>3 3D-modelling</b>	<b>8</b>
<b>4 Space and frequency sounding</b>	<b>11</b>
<b>5 Conclusions</b>	<b>13</b>
<b>References</b>	<b>14</b>

## 1. Introduction

The capability to rapidly characterise the battle environment is crucial to the success of all forward area operations. Hence, rapid environment characterisation (REA) is therefore an area of growing interest to the Swedish Armed Forces. Here we report on an analysis of a field trial designed to test techniques for estimating sub-bottom conductivity profiles. These parameters are vital in the process of calculating the correct propagation of underwater electromagnetic fields. For instance, this information is used in tactical support systems when one is estimating vulnerability to detection for own ships and detection ranges for its sensors.

Among the objectives of the field trial we would like to stress the investigation of three dimensional (3D) effects on the propagation of electromagnetic fields as well as the comparison of space and frequency sounding for the estimation of sub-bottom profiles. During the field trial data were also collected to be able to compare such controlled source EM techniques with traditional magnetotelluric (MT) surveys. The results of the latter comparison will be presented elsewhere.

In order to study the 3D effects of the environment on the propagation of electromagnetic fields the sea trial was performed in an area with moderately varying bathymetry, which also was collected during the exercise. An electromagnetic transmitter was towed along tracks passing near a small island and the transmitted electromagnetic fields were recorded using three-axis electric and magnetic field sensors. The experimental data was compared with the results obtained from 1D and 3D propagation codes [1, 2], respectively. This comparison indicates that 3D effects on the propagation are important when one is trying to model electromagnetic underwater propagation in such areas.

Sub-bottom conductivity profiles have been estimated using data from space sounding as well as frequency sounding. In order to explore the parameter space a local restarted Levenberg-Marquardt optimisation algorithm was used. This provides information on the number of local minima, the corresponding value of the cost function and the number of starting points that end up in each minimum. To investigate seasonal effects, the sub-bottom conductivity profiles estimated from the current data, collected in June 2004, have also been compared with profiles estimated from data collected in the same area in August 2002 [3].

In parallel to the rapid environmental characterisation field trial, data were also collected for E- and B-field background characterisation as well as analysis of how the size of the electrode system (baseline) and the source strength affect the detection range. Together with an analysis of electric and potential field formulations for the long baseline system, this will be reported elsewhere. We will now continue with the description of the field trial.

## 2. The field trial

A short baseline 3-axis electrode system, figure 2, S1, and an electric current dipole were deployed in an area in the southern Stockholm archipelago, figure 1. For the so called frequency sounding part a version of the controlled dipole source, figure 3, was stationary at the positions P1 and P2. For the space sounding and 3D-modelling validation a movable type, figure 4 was towed along the tracks T1 and T2. The electrode sensor and the two kinds of sources are shown in the figures 2-4.

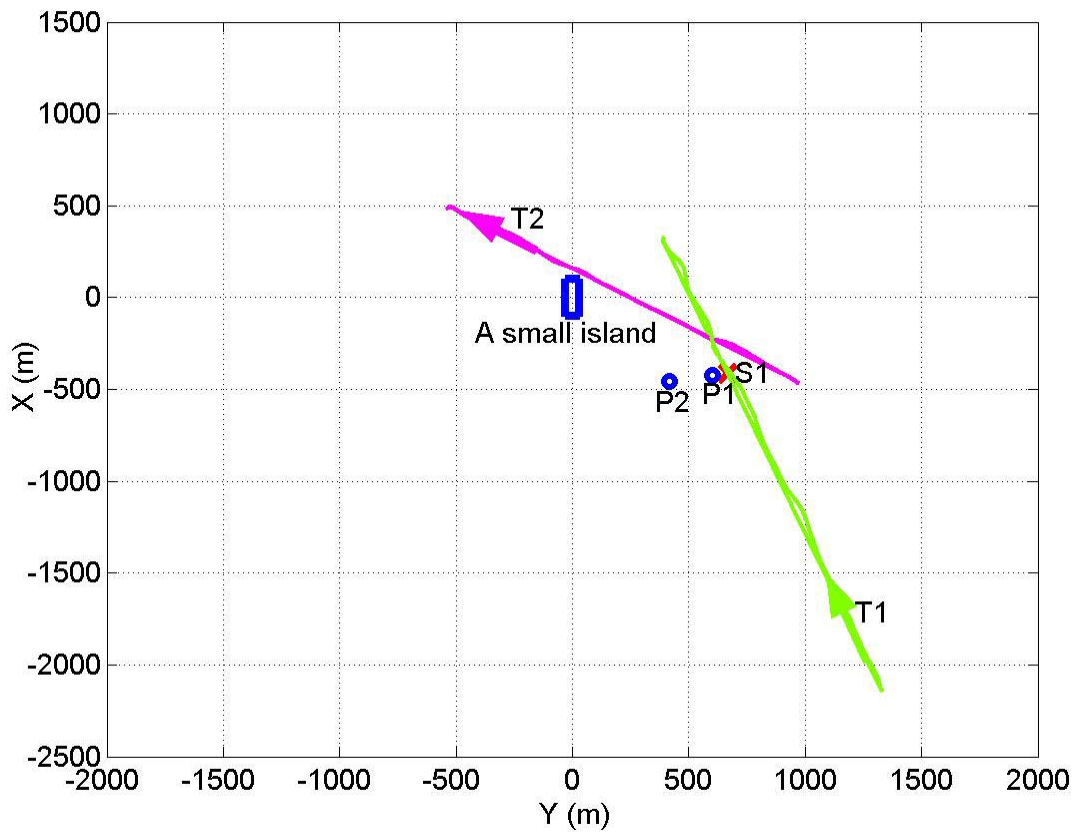


Figure 1. The experimental configuration for the environment characterisation.

The baselines between the horizontal electrode pairs on S1 were 5 m, whereas the vertical baseline was 2 m. Carbon fibre electrodes were mounted at the ends of plastic pipes, which were attached to a concrete slab weighting around 100 kg. Compass and tiltmeters were mounted on the same platform as well as a pod containing electrode amplifiers and electronics for transmission of the signals through cables to land. System S1 was placed on the seafloor at a depth of 24 m.

In order to minimize the signal loss across a cable to land, a so called balanced transmission was applied, in which both the signal itself and the inverted signal are sent on a twisted pair. The amplifier gain was set to 10000 (80 dB) in the frequency range 5 mHz to 11 kHz, and the signals passed anti-aliasing filters with the possibility to add extra gain or attenuation. A 16-bit A/D converter on a PCI-card mounted inside a PC on land was used for the data acquisition.

In the space sounding a 2-pole anti-aliasing filter was set to 100 Hz with a 500 Hz sampling frequency for the resulting electric fields from T1 and T2. The towed source consisted of two copper electrodes, two floating devices, and a system of lines, figure 4. The electrodes were attached to 2.5 m long strings and hung under the floating devices. The effective distance between the electrodes was 10.0 m. The source was towed along the tracks T1 and T2 at a speed of 5 knots. The towing boat was equipped with a DGPS receiver for logging the position as function of time. The source frequencies along T1 and T2 were 5 and 3 Hz, respectively. A dipole moment of 100 Am was used in both cases, in order to achieve a sufficiently high signal-to-noise ratio in the sensor at S1.



*Figure 2. Three-axis short baseline electrode system. Electrodes are at the ends of the grey plastic pipes. The long, thin, yellow rod is one of the magnetic coils. Compass and tiltmeters are in the small pod and amplifiers in the big one.*

In the frequency sounding the anti-aliasing filter and the sampling frequency were set to 1 and 5 kHz, respectively, for transmitted frequencies at P1 and P2 below 1000 Hz. Transmitted electric currents of higher frequencies was sampled at 20 kHz with a anti-aliasing filter at 10 kHz. The stationary source on the seafloor at P1 and P2 consisted of two titanium electrodes mounted at the ends on a 5.5 m long plastic rod, figure 3. The depth of the source at P1 and P2 was 23 and 23.7 m, respectively. Compass and tiltmeters were used to measure the orientation of the source. Sequences of monochromatic currents with frequencies between 1 and 4466 Hz were transmitted for the frequency sounding part described below.

The output current from the sources was produced by a non-commercial control unit. The main constituent of this unit was an amplifier. A programmable function generator (Stanford DS345) was used for signal generation. During all measurements the output current was monitored on an oscilloscope by measuring a voltage drop across a precision resistor connected in series with the electrodes and the water. The output current and voltage from the source were measured by two separate volt meters.





*Figure 3. Stationary electric source with titanium electrodes at each end. The small pod above two of the legs contains compass and tiltmeters.*

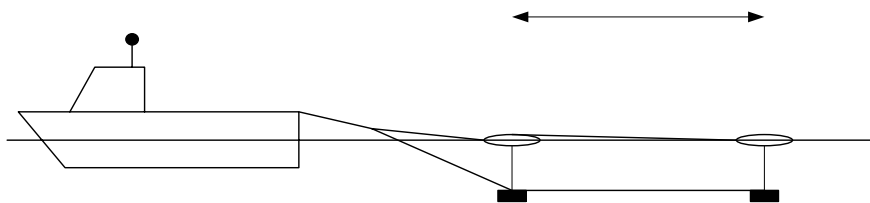


*Figure 4. Basic principle of the towed sources. The polarity is indicated in the figure.*

### **3. 3D-modelling**

Three-dimensional (3D) modeling of the bathymetry and sub-bottom structure is addressed in this section. In particular, the non-planar bathymetry along track T2, figures 1 and 5, is studied with respect to influences on the electric field at S1. The amplitude of the measured electric field is compared with numerical results from the volume integral equation code EMrad [2]. The effects from the bathymetry are highlighted by comparing the data with the corresponding electric field calculated using a horizontally stratified environment as well.

If the bathymetry only varies a few meters over the area of interest, extremely low frequency electric (ELFE) fields from dipole-like sources can be accurately modelled by using a horizontally stratified approximation of the environment. It was shown in [4] that the electric field from a towed dipole source over planar bottom structures can be modelled within a few dB from measured data. In that case, the code Nlayer 2.0, [1], was used with a conductivity profile obtained by space-sounding inversion.

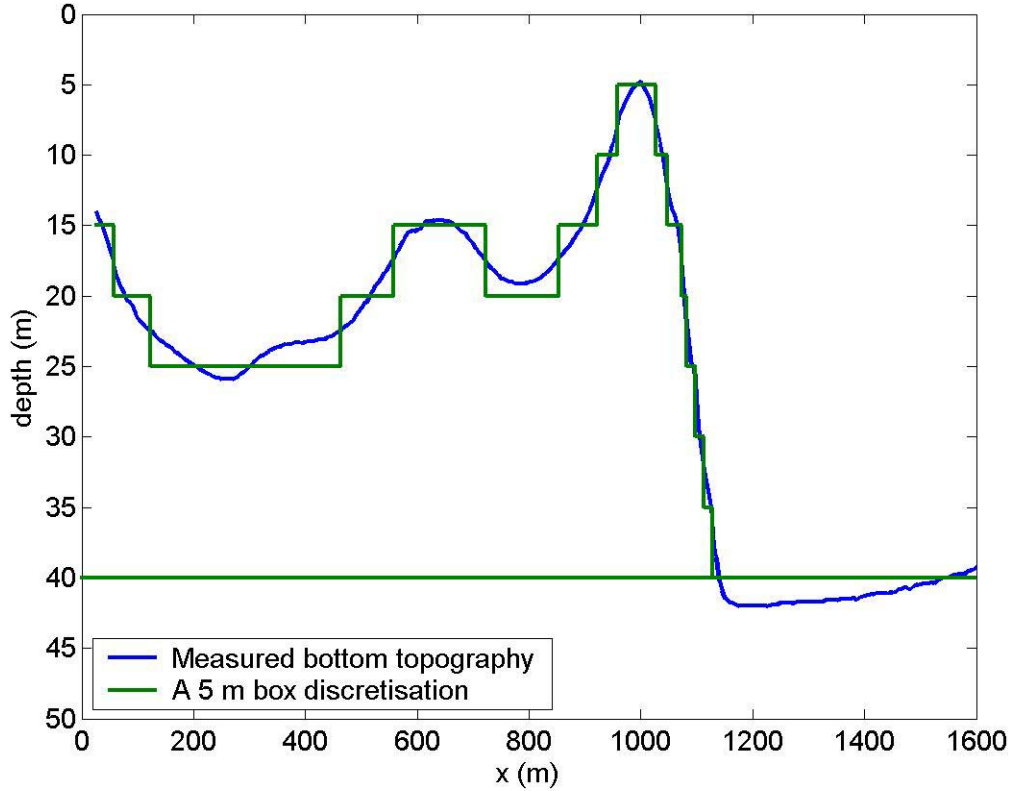


Figure 5. The bathymetry along track T2.

For non-planar bottom structures alternate methods must be considered. Commonly used computational methods for electromagnetic fields from controlled sources within geometries like the one in figure 5, are often based on integral-equation formulations, c.f. [2, 5-9]. In this case, a volume integral representation (1) is derived from the Maxwells equations:

$$\mathbf{E}(\mathbf{r}) = \mathbf{E}^{(lay)}(\mathbf{r}) + \int_V (k^2 - k_b^2) \mathbf{G}_e(\mathbf{r}, \mathbf{r}') \cdot \mathbf{E}(\mathbf{r}') dV(\mathbf{r}'). \quad (1)$$

The electric field at the point  $\mathbf{r}$  from the towed dipole source in the horizontally stratified geometry without the inhomogeneity is given by  $\mathbf{E}^{(lay)}(\mathbf{r})$ , which is computed by Nlayer 2.0 [1]. The contribution to the electric field due to the bathymetry variation is given by the volume integral over  $V$ , where  $V$  is taken as the part of the sub-bottom which differs from the horizontally stratified geometry. Here  $V$  is defined as the part of the sub-bottom above the horizontal green line in figure 5. The effect from the surrounding environment is implicitly incorporated in the dyadic Green's function  $\mathbf{G}_e(\mathbf{r}, \mathbf{r}')$ , c.f. [7]. Its three columns are the normalised electric fields at  $\mathbf{r}$  from three mutually perpendicular electric dipoles at  $\mathbf{r}'$ , i.e. in

the x-, y-, and z-direction. The wave number  $k_b$  relates to the horizontally stratified geometry, whereas  $k$  is the wave number for the volume  $V$ . The unknown electric field  $\mathbf{E}(\mathbf{r}')$  within the volume  $V$  is determined by utilising an extended Born-approximation approach when solving the resulting integral equation. A more thorough mathematical description of EMrad, the numerical implementation of (1), is given in [2].

The background model for T2 yielding the  $\mathbf{E}^{(lay)}(\mathbf{r})$  field, is a three layer model consisting of an infinite layer of air, a 40 m thick seawater layer with a conductivity of 0.75 S/m and an infinite bedrock layer. The bedrock conductivity is estimated to 0.06 S/m by adjusting the background-model data to the measured data at the part of the track where the source passes the sensor, i.e. at the closest point of approach (cpa) to S1. The conductivity in  $V$  is set to the same as value as for the bedrock.

At the present site, along T2, the bathymetry varies according to the blue curve in figure 5. This variation in depth over the 1600 m long track clearly influences the electric field at S1, which is seen in figure 6. The very shallow part of the track 1000 m from the start is seen to cause an increase of the measured electric field with 20 dB relative to the value predicted with Nlayer 2.0 for a flat bottom. The 15 m shoal hump at 700 m also gives rise to a slightly amplified electric field. Hence, the range-dependent marine environment along T2 has to be taken into account, in order to model the variations in the electric field amplitudes.

Here the volume  $V$  is discretised into cubic blocks in the numerical implementation of (1). The side length of each block is chosen to 5 m, which gives a convergent solution of the volume integral with a relative error below 1 %. The extension of  $V$  in the y-direction, i.e. perpendicular to T2, is 180 m. The bathymetry variation in this direction is not taken into account since we could not access any unclassified maps over this region, from which the complete bottom bathymetry data could be extracted. Hence, the water depth above the volume  $V$  is constant in the y-direction. This approximation of the bathymetry essentially affects the component perpendicular to the track of the electric field. The agreement between the measured and modelled electric field in this direction will not be as good as for the in-line component. The main reason is the neglected small island close to the shallow part of T2. The amplitude in the in-line direction is less sensitive to variations in the bathymetry beside the track when the sensor is situated close to the track line.

The 3 Hz transmitted source current and a seawater conductivity of 0.75 S/m, make the dyadic Green's function very much like a Dirac  $\delta$ -function when  $\mathbf{r}$  belongs to  $V$ . Hence, the extended Born approximation gives a good estimate of the electric field inside  $V$  in this case, and further a reliable solution to the electric field at S1. This is visualised in figure 6 where the modelled electric field amplitude matches the measured amplitude very well. The main characteristics of the field along the track are also well captured. The numerical data resulting from the horizontally stratified background model and plotted in light blue in figure 6, do not agree with the measured data when the source comes close to the bottom along the track.

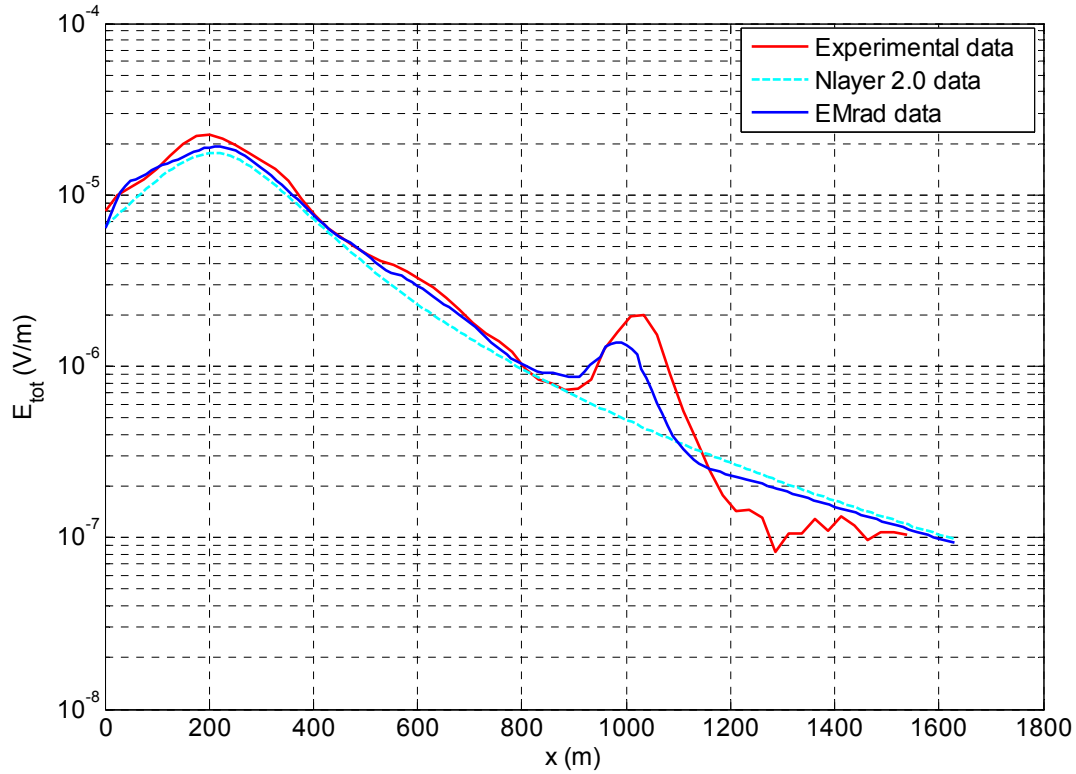


Figure 6. The magnitude of the electric field at sensor S1 when the HED source is towed along track T2.

#### 4. Space and frequency sounding

As shown in the previous section the variations in bathymetry at track T2 had a significant effect on the E-fields at the location of sensor S1. It is therefore difficult to characterise the environment with a horizontally stratified conductivity profile. Compared to the region close to track T2 the bottom is much flatter along track T1. That region has been described as almost horizontally stratified in geological surveys. In 2002 it was demonstrated that it was possible to make accurate electric field predictions in this area, by describing the environment with a range independent conductivity profile [3]. The estimation of the sub-bottom conductivities and layer thicknesses in the environment model was then extracted from frequency and space sounding experiments. A very similar environment characterisation was performed in the present sea trial. The position of the sensor S1 was nearly identical as in the sea trial in 2002. Furthermore, the positions and frequencies of the stationary source at P1 and P2 used for frequency sounding, and the track T1 used for space sounding, were essentially the same. Effective 3-layer models were estimated as well as 9- and 10-layer models. In the 3-layer models, effective water conductivities are determined by inversion together with the depth of the lower plane of reflection and the conductivities for the sediment/bedrock structure. The 9- and 10-layer models are based on an approximate division of the water profile in eight layers, which was extracted from water conductivity measurements at the sea trial. In the 9-layer case, only an effective half-space of sediment/bedrock is estimated. This means that the depth for the interface to this half-space and its conductivity are calculated. Finally, for the 10-layer models three unknowns are estimated from the track data and four unknowns from the fixed position data. In the case with three unknown parameter values, the

sea floor to sediment interface is kept fixed at a position 25 m below the water surface. Conductivity values for the sediment and bedrock are then calculated as well as the position of the sediment to bedrock interface.

All inversions of the conductivities and layer thicknesses in the current analysis are carried out by a restarted local Levenberg-Marquardt algorithm [10]. The results are shown in table 1. In the space sounding for track T1 approximately the same source-position points as in the sea trial 2002 were used. Furthermore, the same frequencies that were used in the frequency sounding inversions in the 2002 field trial were also used in this analysis. The only difference between the analyses is that the total E-field is used in the inversions instead of the separate x- and y-components. For comparison the results from the space sounding and the frequency sounding for source position P1 of the sea trial 2002 is included in the table. Since the frequency sounding for source position P2 was performed with data from another sensor in the 2002 experiment, it is not shown in the results.

3-layer model	Track 1 2004	Track 1 2002	P1 2004	P1 2002	P2 2004
$\sigma_{\text{water}}$ [S/m]	0.94	0.737	0.758	1.11	0.895
$d_{\text{rock}}$ [m]	35.3	38.7	25.4	35.0	29.3
$\sigma_{\text{rock}}$ [S/m]	0.0001	0.0211	0.161	0.0066	0.0144
9-layer model					
$d_{\text{rock}}$ [m]	47.6	35.1	31.9	45.1	35.5
$\sigma_{\text{rock}}$ [S/m]	0.0001	0.0212	0.078	0.0573	0.0040
10-layer model					
$d_{\text{sediment}}$ [m]	25.0 (fixed)	25.0 (fixed)	32.9	41.8	40.2
$\sigma_{\text{sediment}}$ [S/m]	4.96	0.60	0.074	0.15	0.00025
$d_{\text{rock}}$ [m]	28.1	37.3	62.8	63.8	98.4
$\sigma_{\text{rock}}$ [S/m]	0.0001	0.0212	0.71	0.0269	0.042

Table 1. The estimated environment models from the sea trial together with the results from the sea trial 2002.

As seen in table 1, the results from the different sea trials 2002 and 2004 are not very similar. The largest differences are seen in the estimated 10-layer models for the space sounding from track T1. In contrast to the trial 2002 the estimated conductivity of the sediment (4.96 S/m) is not physically realistic, and the conductivity for the rock exceeds its lower boundary (0.0001 S/m) in the searching algorithm. The reason for the extraction of this model could be that the cost function has a trench with several good solutions around the minima. Among these are also models with more realistic parameters. However, even though the environment profile estimated this year and the profile extracted 2002 differ a lot, both profiles seem to approximate the environment reasonably well. In figure 7 the amplitude of the measured electric field in sensor S1 is shown together with the theoretically predicted fields for track T1. The predictions are calculated with Nlayer2.0 and are based on the extracted 10-layer conductivity profiles from the different sea trials. As seen the latest profile works slightly better than the 2002 profile.

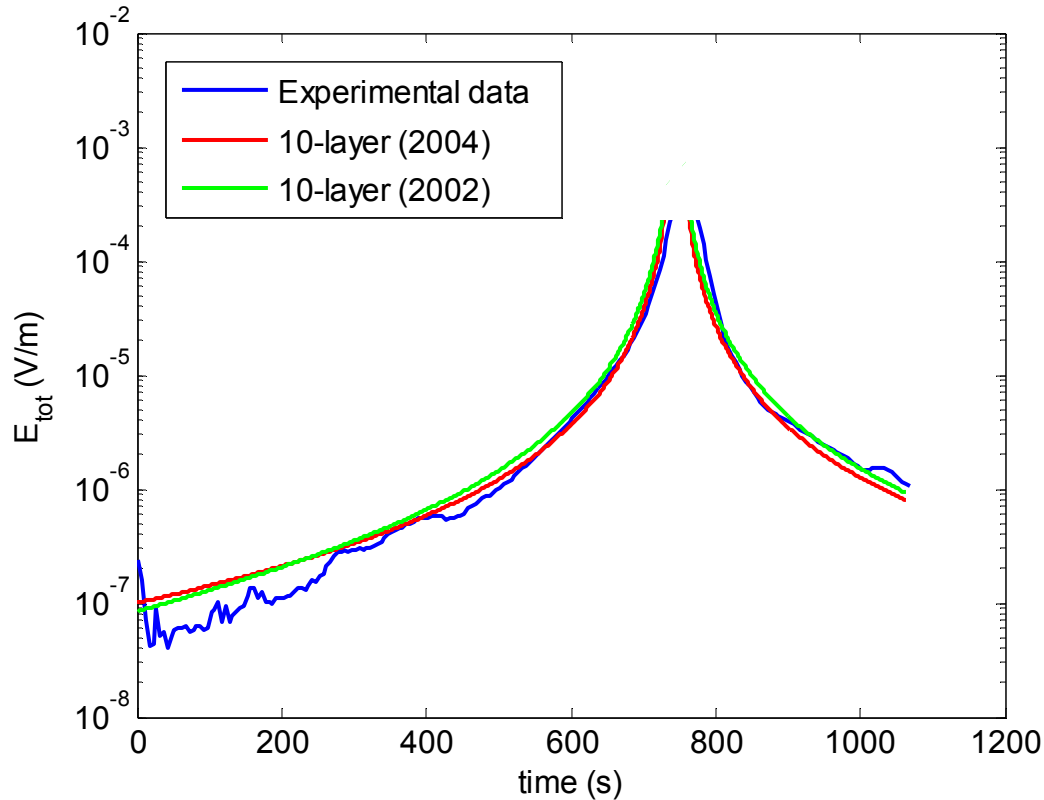


*Figure 7. The amplitude of the measured electric field is compared with the theoretical predicted fields for both the environment profile estimated in this sea trial and the profile extracted in 2002. Note that the sensor is set up to measure very small variations of the E-field and it only measures signals up to a certain threshold. Here this threshold is surpassed when the source passes the sensor and that part of the data has not been included in the picture.*

## 5. Conclusions

An electromagnetic field trial performed in very shallow waters is presented and analysed in this report. Effects on the electric field from an electric dipole source that is towed along a track with a water depth varying between 5-40 m, has been identified and modelled. The very shallow part of the track T2, when the source is just a few meter above the seafloor, increases the electric field amplitude about 20 dB. This effect can be modelled by the EMrad code based on a volume integral equation technique. Since the bathymetry along the track, but not perpendicular to the track, is taken into account the in-line electric field will probably be better modelled than the cross-line electric field component. This should be most prominent when the source is in proximity to the shallow part of the track near the small island. Hence, a detailed study of this range dependent environment is needed. For instance, with a full 3D bathymetry the individual components of the electric field will be more accurately modelled. The next step will be to determine how large variations in the bathymetry that are acceptable before 3D models of the environment are required.

Horizontally stratified models for the sub-bottom conductivity have been obtained by inverting space- and frequency sounding data, respectively. In order to explore possible seasonal dependence in the estimated sub-bottom conductivity profiles the field trial was

planned to resemble a similar field trial performed in August 2002. However, uncertainties in the measured electric field components forced us to estimate sub-bottom profiles based on the amplitude of the electric field. This results in a more ill-posed inverse problem with multi-extremal cost functions. Hence, the differences in the estimated sub-bottom profiles can not solely be linked to seasonal effects based on the current analysis. We therefore recommend trying inversions based on a combination of space and frequency sounding. The additional information should give a less ill-posed inverse problem. We furthermore recommend that the equipment on the sea bottom is left for a long time and that data is collected during different times of the year.

## References

- [1] L. Abrahamsson and B. L. Andersson, *NLAYER – An ELFE code for horizontally stratified media*, FOA-R--97-00586-409--SE, Oct. 1997.
- [2] J. Mattsson, M. Karlsson and J. Schiöld, *Surveillance performance of electric sensors: Effects of range dependent modelling of the electromagnetic environment*, in the proceedings of the conference UDT Europe 2004, 23-25 June 2004, Nice, France.
- [3] P. Krylstedt and J. Mattson, *Environment assessment for underwater electric sensors, in the proceedings of the conference*, UDT Europe 2003, 24-26 June 2003, Malmö, Sweden.
- [4] J. Mattsson, P. Krylstedt and M. Karlsson, *Recovery of the sub-bottom conductivity profile from electromagnetic data collected off the coast of San Diego*, in the proceedings of the conference on marine electromagnetics, MARELEC 2004, March 17-18, London.
- [5] P. E. Wannamaker, G. W. Hohmann and W. A. SanFilipo, *Electromagnetic modeling of three dimensional bodies in layered earths using integral equations*, Geophysics, vol. 49, no. 1, p. 60-74, 1984.
- [6] K. A. Michalski and J. R. Mosig, *Multilayered Media Green's Functions in Integral equation Formulations*, *IEEE Transactions on antennas and propagation*, vol. 45, no. 3, p. 508-519, March 1997.
- [7] C. T. Tai, *Dyadic green functions in electromagnetic theory*, 2nd ed., IEEE PRESS, New-York, 1993.
- [8] J. Mattsson, *NLAYSCA – A computer program for EM-scattering by smooth 3D objects in horizontally stratified media*, FOA-R—99-01092-409—SE, March 1999.
- [9] T. J. Cui, W. C. Chew, A. A. Aydinler and Y. H. Zhang, *Fast-Forward Solvers for the Low-Frequency Detection of Buried Dielectric Objects*, *IEEE transactions on geoscience and remote sensing*, vol. 41, no. 9, Sept. 2003.
- [10] J. Schiöld, *Electromagnetic conductivity profile estimation by quasi-global restarting techniques of local Newton-like methods*, FOI-R—0493—SE, June 2003.